Implications on Inelastic Dark Matter from 100 Live Days of XENON100 Data

E. Aprile,[1] K. Arisaka,[2] F. Arneodo,[3] A. Askin,[4] L. Baudis,[4] A. Behrens,[4] K. Bokeloh,[5] E. Brown,[5] T. Bruch,[4] G. Bruno,[3] J. M. R. Cardoso,[6] W.-T. Chen,[7] B. Choi,[1] D. Cline,[2] E. Duchovni,[8] S. Fattori,[9] A. D. Ferella,[4] F. Gao,[10] K.-L. Giboni,[1] E. Gross,[8] A. Kish,[4] C. W. Lam,[2] J. Lamblin,[7] R. F. Lang,[1] C. Levy,[5] K. E. Lim,[1] Q. Lin,[10] S. Lindemann,[11] M. Lindner,[11] J. A. M. Lopes,[6] K. Lung,[2] T. Marrodán Undagoitia,[4] Y. Mei,[12,9] A. J. Melgarejo Fernandez,[1,*] K. Ni,[10] U. Oberlack,[12,9] S. E. A. Orrigo,[6] E. Pantic,[2] R. Persiani,[13] G. Plante,[1] A. C. C. Ribeiro,[6] R. Santorelli,[1,4] J. M. F. dos Santos,[6] G. Sartorelli,[13] M. Schumann,[4,12] M. Selvi,[13] P. Shagin,[12] H. Simgen,[11] A. Teymourian,[2] D. Thers,[7] O. Vitells,[8] H. Wang,[2] M. Weber,[11] and C. Weinheimer[5]

(The XENON100 Collaboration)

[1]*Physics Department, Columbia University, New York, NY 10027, USA*
[2]*Physics & Astronomy Department, University of California, Los Angeles, USA*
[3]*INFN Laboratori Nazionali del Gran Sasso, Assergi, 67100, Italy*
[4]*Physics Institute, University of Zürich, Winterthurerstr. 190, CH-8057, Switzerland*
[5]*Institut für Kernphysik, Westfälische Wilhelms-Universität Münster, 48149 Münster, Germany*
[6]*Department of Physics, University of Coimbra, R. Larga, 3004-516, Coimbra, Portugal*
[7]*SUBATECH, Ecole des Mines de Nantes, CNRS/In2p3, Université de Nantes, 44307 Nantes, France*
[8]*Department of Particle Physics and Astrophysics, Weizmann Institute of Science, 76100 Rehovot, Israel*
[9]*Institut für Physik, Johannes Gutenberg Universität Mainz, 55099 Mainz, Germany*
[10]*Department of Physics, Shanghai Jiao Tong University, Shanghai, 200240, China*
[11]*Max-Planck-Institut für Kernphysik, Saupfercheckweg 1, 69117 Heidelberg, Germany*
[12]*Department of Physics, Rice University, Houston, TX 77005 - 1892, USA*
[13]*University of Bologna and INFN-Bologna, Bologna, Italy*

arXiv:1104.3121v1 [astro-ph.CO] 15 Apr 2011

The XENON100 experiment has recently completed a dark matter run with 100.9 live-days of data, taken from January to June 2010. Events in a 48kg fiducial volume in the energy range between 8.4 and 44.6 keV$_{\rm nr}$ have been analyzed. A total of three events have been found in the predefined signal region, compatible with the background prediction of (1.8 ± 0.6) events. Based on this analysis we present limits on the WIMP-nucleon cross section for inelastic dark matter. With the present data we are able to rule out the explanation for the observed DAMA/LIBRA modulation as being due to inelastic dark matter scattering off iodine at a 90% confidence level.

PACS numbers: 95.35.+d, 14.80.Ly, 29.40.-n,
Keywords: Dark Matter, Direct Detection, Xenon

Dark matter particles from the Galactic halo are expected to show an annual modulation of the event rate induced by the Earth's motion around the Sun [1]. Such a modulation has in fact been observed in the DAMA/LIBRA experiment [2, 3]. However, this result is difficult to be interpreted as dark matter signals from WIMPs, given the null results from other direct dark matter searches [4]. In order to overcome these tensions, inelastic dark matter (iDM) has been proposed [5–7] as a modification of the elastic WIMP model. iDM assumes that WIMPs scatter off baryonic matter by simultaneously transitioning to an excited state at an energy δ above the ground state ($\chi N \to \chi^* N$), while elastic scattering is forbidden or highly suppressed. This introduces a minimum velocity for WIMPs to scatter in a detector with a deposited energy E_{nr} [8]

$$\beta_{min} = \sqrt{\frac{1}{2M_N E_{nr}}} \left(\frac{M_N E_{nr}}{\mu} + \delta \right),$$

where M_N is the mass of the target nucleus, μ is the reduced mass of the WIMP/target nucleus system and δ is the energy difference between the ground and excited states of the WIMP. In particular, WIMPs with velocities lower than $\sqrt{2\delta/\mu}$ will not be able to scatter at all. Therefore, the available fraction of WIMPs that can interact will be larger for more massive target nuclei, like iodine or xenon.

In contrast to elastic WIMP scattering, where an exponential recoil energy spectrum is expected, the low velocity threshold of the process leads to a spectrum in which the low energy part is suppressed, peaking at recoil energies of 20 keV$_{\rm nr}$ (keV nuclear recoil equivalent) and above. The differential event rate is given by

$$\frac{dR}{dE_{nr}} = N_T M_N A^2 F^2 \frac{\rho_\chi \sigma_N}{2M_\chi \mu^2} \int_{\beta_{min}}^{\infty} \frac{f(v)}{v} dv,$$

where N_T is the total number of nuclei in the target, A is the atomic number of the target nucleus, F is the nuclear form factor, σ_N is the WIMP-nucleon cross section and ρ_χ and M_χ are the WIMP density and mass, respectively. Another consequence of this minimum velocity is the higher sensitivity of the recoil spectrum to the tail of the WIMP velocity distribution, which makes the annual modulation effect larger for inelastic than elastic WIMP scattering.

The XENON100 experiment [9] has just reported results for 100.9 live-days of a dark matter search [10]. The same data are used here to constrain the iDM model. Single scatter events observed in the 48 kg liquid xenon fiducial volume are shown in figure 1. Three events fall in the pre-defined WIMP search region for dark matter interactions, which is compatible with the background expectation described in [10] of (1.8 ± 0.6) events. Hence no significant signal is observed.

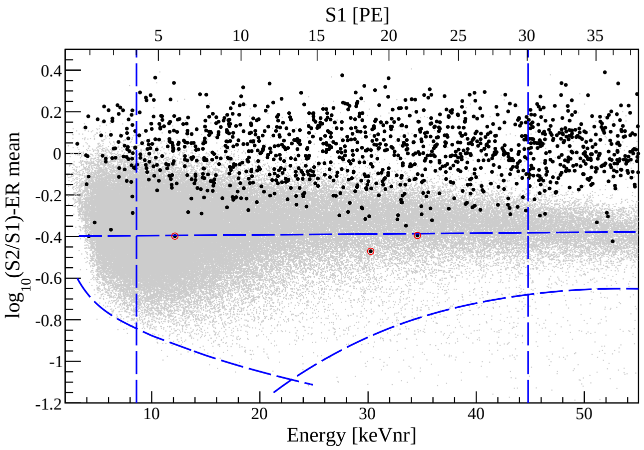

FIG. 1: Events observed in the XENON100 experiment passing all analysis cuts with 100.9 days of data and a fiducial mass of 48 kg. 3 events are found in the predefined WIMP search region.

To extract the DAMA allowed region, the procedure described in [4] has been followed, using a quenching factor of 0.08 for iodine and not considering ion channeling. A χ^2 goodness-of-fit test of the data has been used for computing the lower 90% confidence limit on the cross section σ_N for different values of M_χ and δ. The resulting cross section can be used to predict a scatter rate in XENON100. As an example, figure 2 shows the expected spectrum in XENON100, taking into account exposure and acceptance, and the 90% confidence level cross section from DAMA for different choices of M_χ and δ in the allowed region. The WIMP velocity has been averaged considering the data taking period to account for annual modulation effects.

With this data a limit on σ_N can be extracted for every pair of M_χ and δ values using both the Feldman-Cousins method [11] or the optimum gap method [12]. We assume a Maxwellian WIMP velocity distribution with characteristic velocity $v_0 = 220\,\mathrm{km/s}$ and escape velocity $v_{\mathrm{esc}} = 544\,\mathrm{km/s}$, a local WIMP density of $0.3\,\mathrm{GeV/cm^3}$, Earth's velocity $v_\oplus = 29.8\,\mathrm{km/s}$ [4] and Helm form factors [13]. Figure 3 shows the extracted limit for $\delta = 120$ keV using the Feldman-Cousins method. The DAMA 90% confidence level signal region is also shown in the plot.

The systematic application of the procedure described above to the DAMA data for all the points in the δ-M_χ

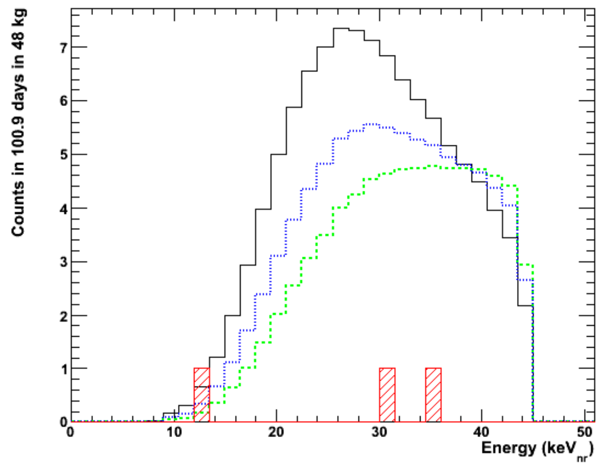

FIG. 2: Expected spectrum in XENON100 in 100.9 live-days between January and June for a WIMP with $M_\chi = 50$ GeV, $\delta = 110\,\mathrm{keV}$ (black, solid); $M_\chi = 55$ GeV, $\delta = 115\,\mathrm{keV}$ (blue, dotted), and $M_\chi = 60$ GeV, $\delta = 120\,\mathrm{keV}$ (green, dashed) and a σ corresponding to the lower 90% confidence limit of the DAMA signal. The XENON100 observed spectrum is shown in red

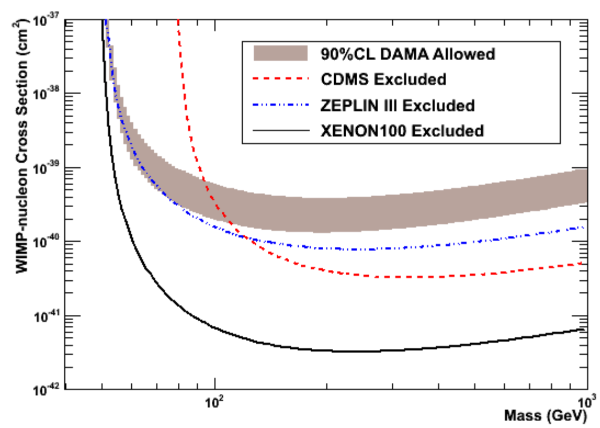

FIG. 3: DAMA 90% confidence level signal region for $\delta = 120$ keV. Superimposed are the 90% confidence level exclusion curves for XENON100 (black, solid), CDMS [14] (red, dashed) and ZEPLIN-III [15] (blue, dash-dotted). The whole DAMA WIMP region is excluded by XENON100.

space results in the gray area in figure 4, which shows the allowed parameter space. Previous constraints on iDM from CDMS [14, 16], CRESST [17] or EDELWEISS-II [18] results involved target nuclei with different masses than iodine, which thus sample a different region of the WIMP velocity distribution. Thanks to the similar mass of xenon and iodine nuclei, constraints inferred from liquid xenon experiments are robust with respect to uncertainties in halo parameters. This has already been shown by ZEPLIN-III [15], which however leaves a very small fraction of the spectrum available for iDM due to the limited exposure. The whole DAMA parameter space is incompatible with the XENON100 data at 90% confidence level. This result is independent of the statistical method used to analyze the data.

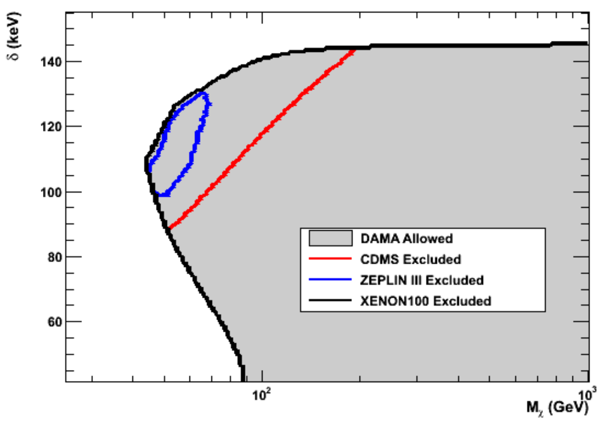

FIG. 4: Parameter space to explain the DAMA annual modulation with iDM (bounded area), and parameter space excluded by different experiments. The black line corresponding to XENON100 excludes the whole DAMA allowed region. $v_0 = 220\,\mathrm{km/s}$ and $v_{esc} = 544\,\mathrm{km/s}$ have been used. CDMS [14] (red) and ZEPLIN-III [15] (blue) exclusion curves are also shown.

Due to the cutoff at low energies associated with the iDM interactions, the results can strongly depend on the chosen astrophysical parameters. To ensure the robustness of the present result, the calculations have been repeated for $v_{esc} = 500\,\mathrm{km/s}$ and $v_{esc} = 600\,\mathrm{km/s}$. The conclusion remains unchanged.

We gratefully acknowledge support from NSF, DOE, SNF, Volkswagen Foundation, FCT, Région des Pays de la Loire, STCSM, DFG, Minerva Gesellschaft and GIF. We are grateful to LNGS for hosting and supporting XENON.

* Electronic address: ajmelgarejo@astro.columbia.edu

[1] A. K. Drukier, K. Freese, and D. N. Spergel, Phys. Rev. **D33**, 3495 (1986).

[2] R. Bernabei et al. (DAMA), Eur. Phys. J. **C56**, 333 (2008), 0804.2741.

[3] R. Bernabei et al., Eur. Phys. J. **C67**, 39 (2010), 1002.1028.

[4] C. Savage, G. Gelmini, P. Gondolo, and K. Freese, JCAP **0904**, 010 (2009), 0808.3607.

[5] S. Chang, R. F. Lang, and N. Weiner, Phys. Rev. Lett. **106**, 011301 (2011), 1007.2688.

[6] D. Tucker-Smith and N. Weiner, Phys. Rev. **D64**, 043502 (2001), hep-ph/0101138.

[7] D. Tucker-Smith and N. Weiner, Phys. Rev. **D72**, 063509 (2005), hep-ph/0402065.

[8] S. Chang, G. D. Kribs, D. Tucker-Smith, and N. Weiner, Phys. Rev. **D79**, 043513 (2009), 0807.2250.

[9] E. Aprile et al. (XENON100), Phys. Rev. Lett. **105**, 131302 (2010), 1005.0380.

[10] E. Aprile et al. (XENON100) (2011), 1104.2549.

[11] G. J. Feldman and R. D. Cousins, Phys. Rev. **D57**, 3873 (1998), physics/9711021.

[12] S. Yellin, Phys. Rev. **D66**, 032005 (2002), See also S. Yellin (2007), *Extending the optimum interval method*, arXiv:0709.2701, physics/0203002.

[13] R. H. Helm, Phys. Rev. **104**, 1466 (1956).

[14] Z. Ahmed et al. (CDMS) (2010), 1012.5078.

[15] D. Y. Akimov et al. (ZEPLIN-III), Phys. Lett. **B692**, 180 (2010), 1003.5626.

[16] Z. Ahmed et al., Science **327**, 1619 (2010), 0912.3592.

[17] K. Schmidt-Hoberg and M. W. Winkler, JCAP **0909**, 010 (2009), 0907.3940.

[18] E. Armengaud et al. (EDELWEISS) (2011), 1103.4070.